TOXICOLOGICAL SCIENCES **128(1)**, 186–197 (2012)
doi:10.1093/toxsci/kfs150
Advance Access publication April 26, 2012

Gold Nanoparticles Uptake and Cytotoxicity Assessed on Rat Liver Precision-Cut Slices

Stefania Dragoni,* Giulia Franco,* Marì Regoli,† Monica Bracciali,‡ Vittorio Morandi,§ Giampietro Sgaragli,* Eugenio Bertelli,† and Massimo Valoti*,[1]

**Dipartimento di Neuroscienze, Università di Siena, 53100 Siena, Italy and Istituto Toscano Tumori, 50139 Firenze, Italy; †Dipartimento di Fisiopatologia e Medicina Sperimentale, Università di Siena, 53100 Siena, Italy; ‡CABRO spa, 52100 Arezzo, Italy; and §CNR-IMM, Sezione di Bologna, 40129 Bologna, Italy*

[1]To whom correspondence should be addressed at Dipartimento di Neuroscienze, Università di Siena, via Aldo Moro 2, 53100 Siena, Italy. Fax: +390577234446. E-mail: massimo.valoti@unisi.it.

Received July 8, 2011; accepted April 13, 2012

A major obstacle in the field of nanotoxicology is the development of an *in vitro* model that accurately predicts an *in vivo* response. To address this concern, rat liver precision-cut slices were used to assess the impact of 5-nm gold nanoparticles (GNPs) coated with polyvinylpyrrolidone (PVP) on the mammalian liver, following exposure to different concentrations and for a duration of up to 24 h. The presence of GNPs inside endocytotic vesicles of hepatocytes was appreciable within 30 min of their addition. After 2 h, GNPs were clearly visualized inside endosome-like vesicles within the slice, not only in hepatocytes but also in endothelial and Kupffer cells located within the first two cellular layers. This uptake did not translate into modifications of either phase I or phase II of 7-ethoxycoumarin metabolism or alter activities of cytochrome P450 toward marker substrates. Furthermore, although the GNPs were rapidly internalized, no overt signs of cytotoxicity, assessed through lactate dehydrogenase release, reduction of methylthiazolyldiphenyl tetrazolium bromide, and glutathione levels, were observed. In conclusion, the use of rat liver slices successfully enhanced nanomaterial screening and determined that PVP-coated 5-nm GNPs were biocompatible with rat liver cells.

Key Words: **nanoparticles; uptake; nanotoxicity; endocytosis.**

Nanotechnology research and development has been rapidly growing worldwide for the past decade. Due to their extremely small size, nanomaterials (NMs) have a much greater surface area than the same mass of materials at microscale size. At nanoscale size, quantum effects are more important in determining the properties and characteristics of the material. Although NMs provide great potential of commercial benefits, some of them have been claimed to be toxic in *in vivo* and *in vitro* tests (Yang *et al.*, 2009); indeed, at present, our knowledge on their toxicological properties is far from being comprehensive (Lewinski *et al.*, 2008; Savolainen *et al.*, 2010). The potential impact on human health and environment of NMs depend strongly on their physicochemical characteristics. Although up to now there is insufficient evidence to suggest that the development and use of NMs represent substantial health and environmental risks, the rapid boost in the synthesis of new compounds, also shaped in different geometric forms, requires a parallel increase in the understanding of the risks promoted by them. In general, with the current technological capabilities, engineering new nanoparticles (NPs) is a far more rapid task than assessing their toxicity. In other words, toxicological and environmental risk assessment of NPs struggles to keep up with the development of all newly synthesized NMs. To make things even more complex, there is increasing evidence that the chemical composition of NPs is not the only parameter that should be considered for the assessment of their toxicity; as a matter of fact, nanotoxicity depends also on their size and geometric shape (Tarantola *et al.*, 2011; Yang *et al.*, 2009).

Thus, due to the large variance of NPs, several authors have underlined the need of developing reliable *in vitro* models for studying the toxic effects of NPs. Indeed, Lee *et al.* (2009) have highlighted that 2D cell cultures do not accurately predict NM toxicity *in vivo* because of the absence of several anatomical barriers (Griffith and Swartz, 2006), such as epithelia, that can physiologically represent an effective impairment to the diffusion of NPs. Also, essential behaviors of NPs (and other substances) are neglected with respect to cell functions that are strongly dependent on 3D organization. In particular, as far as the liver is concerned, simple cell cultures of hepatocytes bring NPs in contact with cell domains that *in vivo* are not likely to interact with the particles. For instance, although *in vivo* the basal domain of hepatocytes (vascular domain) comes in contact with NPs circulating in the blood, the same is not applicable to their apical domain (biliary domain).

We have evaluated the uptake of 5-nm gold nanoparticles (GNPs) by liver cells and their toxicity toward liver cells, *in vitro* by using rat liver "precision-cut" slices (de Graaf *et al.*, 2010) incubated with GNPs and *in vivo* by administering GNPs intraperitoneally to rats. We decided to assess the toxicity of GNPs on liver because this organ is one of the major filters

in the mammalian body, which is set along the blood circulatory system and which captures circulating exogenous NPs (Semmler-Behnke *et al.*, 2008), regardless of the route of entry and the chemical and physical structure of NPs (i.e., gold or silica NPs, quantum dots, and nanotubes) (Balasubramanian *et al.*, 2010; Kumar *et al.*, 2010; Schipper *et al.*, 2008).

The presence of all the liver-specific cell types in these slices makes possible the study of liver functions *in vitro* in a multicellular context, which allows to test cell processes and interactions in a "milieu" closely resembling the *in vivo* conditions. Indeed, a number of studies carried out on liver slices have demonstrated that the interactions between Kupffer cells and hepatocytes are preserved (Olinga *et al.*, 2001). Furthermore, the presence of the extracellular matrix, otherwise absent in hepatocyte 2D-cell culture, ensures the coherence of the tissue and the regulation of cell functions by associated growth factors, cytokines, and hormones (Hui and Friedman, 2003; Mohammed and Khokha, 2005).

This study demonstrates that PVP-coated 5-nm GNPs are biocompatible with liver cells. Moreover, we suggest that the liver precision-cut slice model could represent a reliable system for assessing the uptake of NPs and their toxicity toward both the hepatocytes and the other cell types present in liver.

MATERIALS AND METHODS

Chemicals

$HAuCl_4$ (99.5% purity) was synthesized by CABRO spa, Arezzo, Italy. RPMI 1640 was purchased from CAMBREX (Milan, Italy). Polyvinylpyrrolidone (PVP), average molecular weight of 10,000 Da, $NaBH_4$, trisodium citrate, NADPH, NADP, glucose-6-phosphate dehydrogenase, and silver enhancer kit were provided by Sigma-Aldrich (Milan, Italy). All other chemicals and solvents were of the highest grade available and obtained from common commercial sources.

Synthesis and Characterization of GNPs

GNPs were synthesized in CABRO spa laboratory according to the procedure outlined by Turkevich *et al.* (1951), with slight modifications. $HAuCl_4$ (50 ml, 0.1M, 99.8% purity) was quickly added under continuous stirring to a solution containing both $NaBH_4$ (1.5mM) and trisodium citrate (0.2M) and also PVP (5mM) as reducing and protecting agents, respectively. The temperature was then raised up to the boiling point, and the solution was kept at this temperature under reflux and was stirred continuously for 20 min. After cooling to room temperature, reversible aggregation of the GNPs was promoted by adding solid potassium carbonate. The golden powder recovered after centrifugation was dried and then suspended in methanol at the final gold concentration of 86 mg/ml (0.44M). This colloid was stable for several months, without any significant agglomeration. The purity of GNPs was assessed by inductively coupled plasma optical emission spectroscopy (ICP-OES) of ultrafiltrated samples (iCAP 6000 Series ICP Spectrometer; Thermo Scientific, Rodano, Milan, Italy). The morphology and size of GNPs were determined through transmission electron microscopy (TEM) by using FEI-Tecnai F20 equipped with a Schottky emitter and operated at an accelerating voltage of 200 keV. GNPs were examined after suspension in water and subsequent drop casting over conventional TEM holey carbon grids. Dynamic light scattering (DLS) analysis was performed on a DelsaNano device (Beckman Coulter, Milan, Italy) in order to evaluate the size of GNPs after their incubation in different media. The device was equipped with dual 30-mW laser diodes that were set at 658-nm emission wavelength.

Animals

All experiments were performed in strict compliance with the recommendation of the EEC (86/609/CEE) for the care and use of laboratory animals, and the protocols were approved by the Animal Care and Ethics Committee of the University of Siena, Italy. Male Wistar albino rats (250 g; Charles River Italia, Calco, Italy) were kept in large cages under a 12:12 h day-night cycle at 20°C (ambient temperature) with free access to drinking water and conventional laboratory rat food. The rats were fasted overnight prior to the experiment. On the day of the experiment, rats were anesthetized with an ip injection of xylazine chloride (10 mg kg^{-1}; Rompun vet., Bayer AG, Germany) and ketamine hydrochloride (35 mg kg^{-1}; Ketavet, Parke Davis/Warner-Lambert), decapitated, and bled.

In *in vivo* experiments, rats were treated ip with a suspension of 10 mg/kg body weight GNPs and were killed after 12 h. In another series of experiments, the bile duct of rats was cannulated under deep anesthesia 6 h after ip treatment, and the bile was collected up to 12 h.

Liver Precision-Cut Slices Preparation

Livers of the rats were removed, stored in a physiological solution at 4°C, and subsequently placed in an ice-cold Krebs-Henseleit (KH) buffer. Slices were prepared in oxygenated ice-cold KH buffer, using a Krumdieck slicer according to a procedure described elsewhere (de Graaf *et al.*, 2010). Slices (250 μm thick) were incubated at 37°C in 12-well culture plates containing 750 μl of RPMI 1640 supplemented with 5% fetal calf serum, 0.5mM L-methionine, 1μM insulin, 50 μg/ml gentamicin, and 0.1mM hydrocortisone 21-hemisuccinate (de Graaf *et al.*, 2010). The plates were continuously shaken horizontally at 100 rpm. Following an initial 30-min preincubation aimed at equilibrating the slices, the medium was replaced with a fresh vehicle containing GNPs (5–500μM) and incubated up to 24 h. At the end of each experimental session, the slices and incubation media were collected in pairs; when necessary, the slices were homogenized in PBS, pH 7.4, in order to evaluate some biochemical parameters.

ICP-OES

ICP-OES analysis was performed on both the entire liver and the bile collected for 6 h from rats treated *in vivo* (10 mg × kg^{-1} body weight, ip) and on "precision-cut" liver slices incubated with GNPs. The liver obtained from rats treated *in vivo* was homogenized in "ultrapure" water (1:5; v:v) and subsequently digested in *aqua regia*. The gold content of the digestion solution was measured by ICP-OES analysis. Two rats were treated with the same dose of GNPs, and the bile was collected and analyzed by ICP for its gold content.

After 24-h incubation in RPMI containing GNPs at 50 and 500μM concentration, the slices were washed thrice with RPMI not containing GNPs and digested in 500 μl of freshly prepared "optima grade" *aqua regia*. The sample remained immersed in *aqua regia* for 3 h. A 400-μl aliquot of the digestion solution was diluted with "ultrapure" water and analyzed by ICP-OES. This analysis was performed using an iCAP 6000 ICP optical emission spectrometer (Thermo Scientific).

Biochemical Parameters

Lactate dehydrogenase and methylthiazolyldiphenyl tetrazolium bromide assays. In order to evaluate slice viability, lactate dehydrogenase (LDH) leakage and methylthiazolyldiphenyl tetrazolium bromide (MTT) reduction were determined. LDH activity was assessed either in conditioned media or in slice homogenates as previously described (Gay *et al.,* 1968), and the amounts

detected in the medium were reported as percentage of the total content (media + homogenates). MTT reduction assay was carried out as previously reported (Moronvalle-Halley *et al.,* 2005) with slight modifications. Briefly, the slices were incubated in the presence of MTT (0.5 mg/ml) for 1 h at 37°C, thoroughly washed with PBS, and resuspended in 5 ml dimethylsulfoxide in order to dissolve the reduced MTT, and the absorbance of the solution was measured at 570 nm. The values recorded in experimental samples were reported as percentage of those found in control preparations.

Glutathione assay. Oxidative stress was evaluated by measuring glutathione (GSH) concentration as previously reported (Vickers, 2009) with slight modifications. In order to precipitate proteins, aliquots of slice homogenates in PBS containing 0.02M EDTA were combined 1:1 with 10% TCA and centrifuged for 15 min at 3000 g. Fifty microliters of the supernatant was added to 950 µl of 0.4M Tris-HCl, 0.2M EDTA, pH 8.9, containing 3mM DTNB (Ellman's reagent). After 10-min incubation, the absorbance values, determined at 412 nm, were expressed as nmol/mg of proteins and compared with a standard curve achieved using GSH (0–250µM). Oxidized glutathione (GSSG) was determined analogously to the total GSH, except that GSH was first depleted through reaction with an excess amount of N-ethylmaleimide (Onderwater *et al.*, 2004).

Cytochrome P450–dependent activity. The impact of GNPs on the metabolic performance of hepatocytes was assessed by evaluating the efficiency of xenobiotic metabolizing systems. This was accomplished by measuring (1) cytochrome P450–dependent activity on microsomal fractions of slice homogenates prepared by differential centrifugation as previously reported (Dragoni *et al.*, 2007) and (2) glucuronyl- and sulfotransferase activities on precision-cut slices with the use of the appropriate substrate markers.

The pellet retaining the microsomal fraction was suspended in 0.01M Tris-HCl buffer (pH 7.4) containing 0.154M KCl and 1mM EDTA at a final protein concentration of 10 mg/ml. Ethoxyresorufin O-deethylase (EROD), pentoxyresorufin O-depentylase (PROD), and benzoyloxyresorufin O-debenzoylase (BROD) activities were determined by measuring spectrofluorometrically the kinetics of resorufin formation (Dragoni *et al.*, 2007).

7-Ethoxycoumarin metabolism. After 24-h incubation with GNPs, the slices were transferred and incubated for 2 h in a new plate containing a culture medium supplemented with 7-ethoxycoumarin at a final concentration of 50µM. The medium was divided into three aliquots: one aliquot was diluted with 0.5M sodium acetate buffer (pH 5) and used to assess the content of free 7-hydroxycoumarin (CYP(s)-dependent metabolite), whereas the other two were employed to determine the levels of 7-hydroxycoumarin glucuronide and 7-hydroxycoumarin sulfate by adding β-glucuronidase (5000 U/ml) or α-arylsulfatase (250 U/ml). After 16 h of incubation at 37°C, samples were diluted with a buffer solution containing 50mM KCl, 0.154M Tris-HCl, pH 7.4. Thereafter, 100 µl of 4M HCl were added to the reaction mixture before extraction with chloroform and centrifugation for 5 min at 3000 g. Finally, 30mM sodium borate (pH 9.2) was added to the organic phase, and after centrifugation, the aqueous phase was analyzed fluorometrically for its 7-hydroxycoumarin content at excitation and emission wavelengths of 370 nm and 455 nm, respectively. The 7-hydroxycoumarin calibration curve was obtained using increasing concentrations of the analyte (0–0.4µM). The enzyme activities were expressed as pmol metabolite/min/mg of protein.

Histological Analysis

Slices of liver were incubated with two different concentrations of GNPs (50 or 500µM) for various lapses of time (0.5, 1, 2, 3, 4, 6, and 24 h). At the end of the incubation, samples were rinsed thrice for 5 min with fresh medium and then fixed with Karnovsky's fixative in 0.1M cacodylate buffer (pH 7.35) for 1 h. After several washings with the same buffer, slices were *en bloc* silver enhanced with a silver enhancer kit following manufacturer's instructions, fixed again in Karnovsky's fixative for an additional hour, and postfixed for 1 h with 0.1% osmium tetroxide dissolved in 0.1M cacodylate buffer. For a better resolution, the silver enhancement step was omitted in some experiments. In order to assess whether the silver enhancement procedure was affected by free PVP or Au^{+3} possibly released from GNPs, additional slices (negative controls) were incubated in the medium containing 500µM PVP or 500µM $AuCl_3$. The PVP concentration used in this experiment was much higher, even by three orders of magnitude, than the amount used for coating GNPs, which being less than 1% (w/w) of the total mass of GNPs upon complete release from NPs should give rise to less than 100nM concentration.

For *in vivo* experiments, animals were perfused via thoracic aorta with 20 ml of fixative (4% paraformaldehyde and 1% glutaraldehyde in 0.1M cacodylate buffer). Livers were removed, cut into small pieces, and further fixed for 2 h in the same fixative. After rinsing with 0.1M cacodylate buffer, the samples were postfixed for 2 h in 1% osmium tetroxide in the same buffer. Finally, the samples were dehydrated and embedded in Epon 812 according to standard procedures.

Resin blocks containing liver slices were cut along a plane orthogonal to their surface. All samples were cut with an LKB ultramicrotome and ultrathin sections, stained with uranyl acetate and lead citrate, and examined with a Philips 201 TEM.

Statistical Analysis

All the experiments were performed by using at least three liver slices derived from three different rats. Data are reported as mean ± SEM, and n is the number of samples.

Statistical analysis was performed by using Student's t-test or one-way ANOVA followed by *post hoc* Tukey's test as appropriate; $p < 0.05$ was considered significant.

RESULTS

Characterization of GNPs

Evaluation of several TEM images indicated that the GNPs have an average diameter of 5 nm (see also the Supplementary material for the size distribution histogram of GNPs). Furthermore, TEM reflection data and ICP-OES analysis confirmed that the crystalline structure of GNPs was compatible with an Au lattice, and the percentage of Au present in GNPs resulted to be 99.1%. GNPs (see Supplementary material), once they had been coated with PVP in methanol, were dried and suspended, with sonication at nominal 5–500µM concentration (as average number of Au atoms), corresponding to 0.98 and 98 µg gold × ml^{-1} water or culture medium. These suspensions were subjected to dynamic light scattering, which showed that the average diameter of GNPs differed according to the suspension vehicle used, resulting 15.7 nm in methanol, 23.7 nm in water, and 10.9 nm in the culture medium, respectively. GNPs in these suspensions exhibited a great variance in the polydispersion index (PI) ranging from 0.02 in methanol to 0.298 in RPMI. Furthermore, 24-h incubation of NPs in RPMI did not affect their average diameter, whereas PI reached 0.330 value (see Table 1). In contrast, because the Z-potential of GNPs was –20.03 mV in water and –9.74 mV in the culture medium, GNPs were more dispersed in the latter medium, probably owing to the solvation effect of proteins, as already reported (Ponti *et al.*, 2009). The highest concentration used in the present experiment (500µM; 98 µg × ml^{-1} in gold) corresponded to a GNP concentration of 0.12µM as defined by Liu *et al.* (2007) and confirmed by the UV-visible spectrophotometric analysis, as proposed by the same authors.

TABLE 1
Size Characterization of PVP-Coated GNPs Suspended in Different Media

Medium	Hydrodynamic diameter (nm)	Polydispersion index
Methanol[a]	15.7	0.012
Water[a]	23.6	0.154
RPMI (500μM)[a]	10.9	0.298
RPMI (50μM)[b]	11.8	0.330
RPMI (500μM)[b]	10.4	0.329

[a]GNPs coated with PVP were assayed after suspension in methanol and water at 0.44M concentration or in RPMI at 500μM concentration (0-h incubation time).

[b]GNPs coated with PVP were incubated in RPMI at 37°C under a water-saturated atmosphere of 95% CO_2 and 5% O_2 for 24 h and subsequently subjected to dynamic light scattering analysis.

Toxicological Profiles

The release of LDH from liver slices was similar under all the experimental conditions used. In control conditions, the release of LDH was 20.7 ± 2.4 % after 2 h of incubation and reached 35.7 ± 2.7% after a 24-h incubation period. In the presence of GNPs, the highest release of LDH was observed at a concentration of 50μM after 2 h of incubation (25.3 ± 1.7), whereas after 24 h a value of 45.6 ± 7.0% was attained at 300μM concentration; for the other concentrations tested, the release of LDH ranged from 31.6 ± 2.8% to 43.4 ± 11.5%. (100 and 200μM concentration, respectively) (Supplementary fig. S3).

Similar results were observed when the reduction of MTT was monitored. As reported in Figure 1, at all the incubation times, treatment with GNPs at various concentrations did

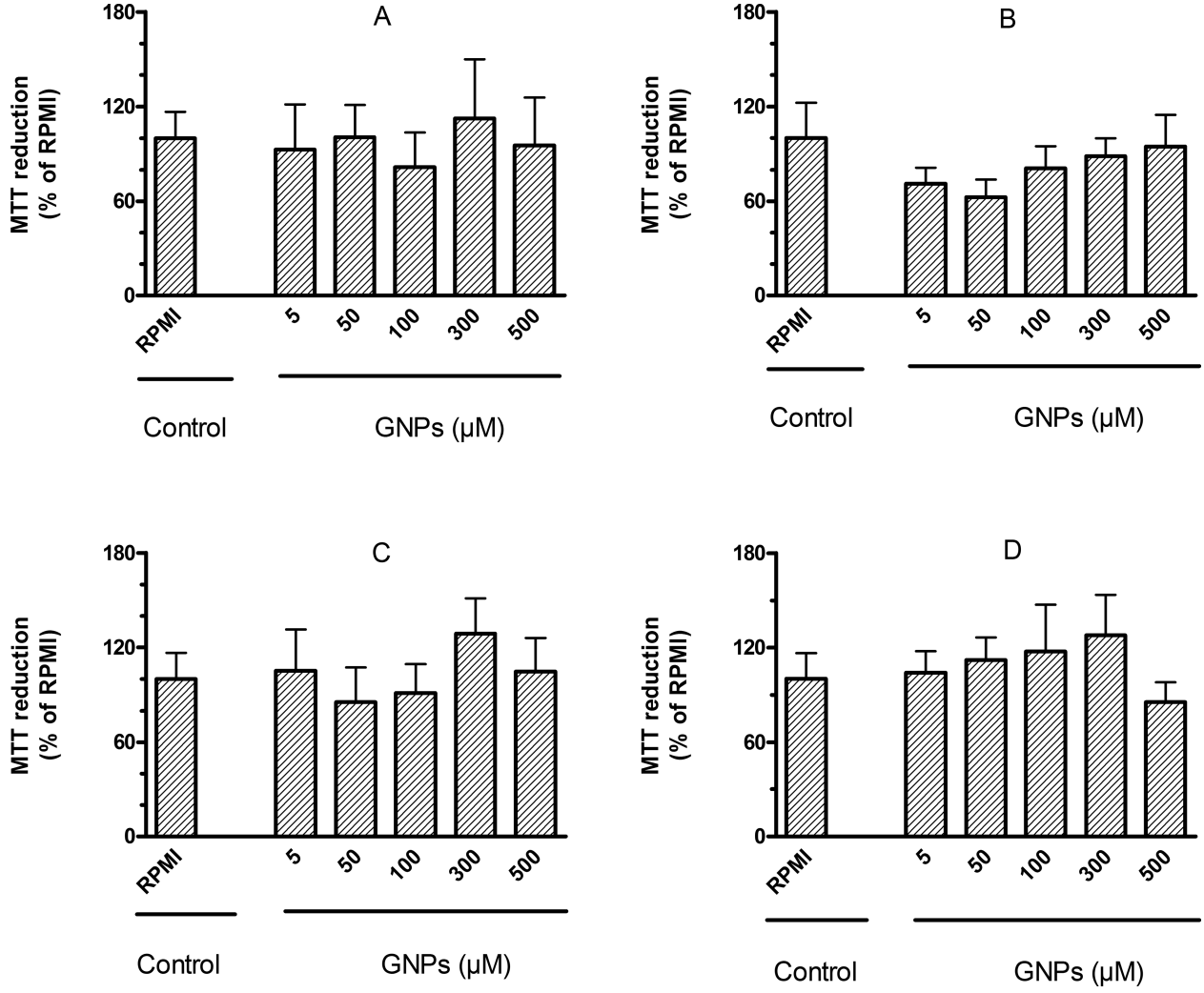

FIG. 1. MTT reduction capability of rat liver precision-cut slices in the presence of GNPs. Slices were incubated for various periods of time (2, 4, 6, and 24 h) in the presence of different concentrations of GNPs (5–500μM) (panel A, B, C, and D, respectively) and then incubated with MTT as reported in the Materials and Methods section. Columns marked RPMI represent slices cultured in the presence of RPMI alone as control conditions. Results are expressed as mean ± SEM of values obtained from three slices per liver ($n = 3$).

not modify the levels of MTT reduction, thus suggesting that GNPs did not affect appreciably the cell viability of liver slices. Furthermore, these results indirectly indicate that GNPs did not alter mitochondrial functions.

Although the metallic nature of the NPs here employed may increase the production of reactive oxygen species (ROS), leading to oxidative stress (Jia *et al.*, 2009; Li *et al.*, 2010), GSH contents of slices incubated with different concentrations of GNPs (Fig. 2) were comparable to those of control slices. A time-dependent decrease of GSH content could be observed, however, under both experimental conditions. Furthermore, the amounts of GSSG in control slices both at 0 h and after 24 h incubation were comparable (1.08 ± 0.46 and 0.88 ± 0.10 nmol × mg proteins^{-1}, respectively) and were not different from the amounts found in slices after 24 h incubation with GNPs at the two concentrations employed (see Table 2).

Metabolic Features of Liver Slices

Ethoxycoumarin O-deethylation is an oxidation reaction catalyzed by different cytochrome P450 isozymes (ECOD; predominantly CYP1A, 2A, 2B, 2C subfamilies). The resulting metabolite, 7-hydroxycoumarin, subsequently undergoes a conjugation reaction with the formation of glucuronyl and/or sulfate derivatives. These metabolic properties make it a suitable substrate for investigating the influence of chemicals on the liver metabolizing system of xenobiotics. The effects of GNPs, at the highest concentration used in this study (500μM), were thus assessed on 7-ethoxycumarin metabolism by liver slices. As shown in Figure 3, the slice levels of free 7-hydroxycoumarin and those of 7-hydroxycoumarin glucuronide and 7-hydroxycoumarin sulfate were comparable both in the presence or in the absence of GNPs, indicating that either CYPs or conjugative enzyme-dependent activities were unaffected by GNPs.

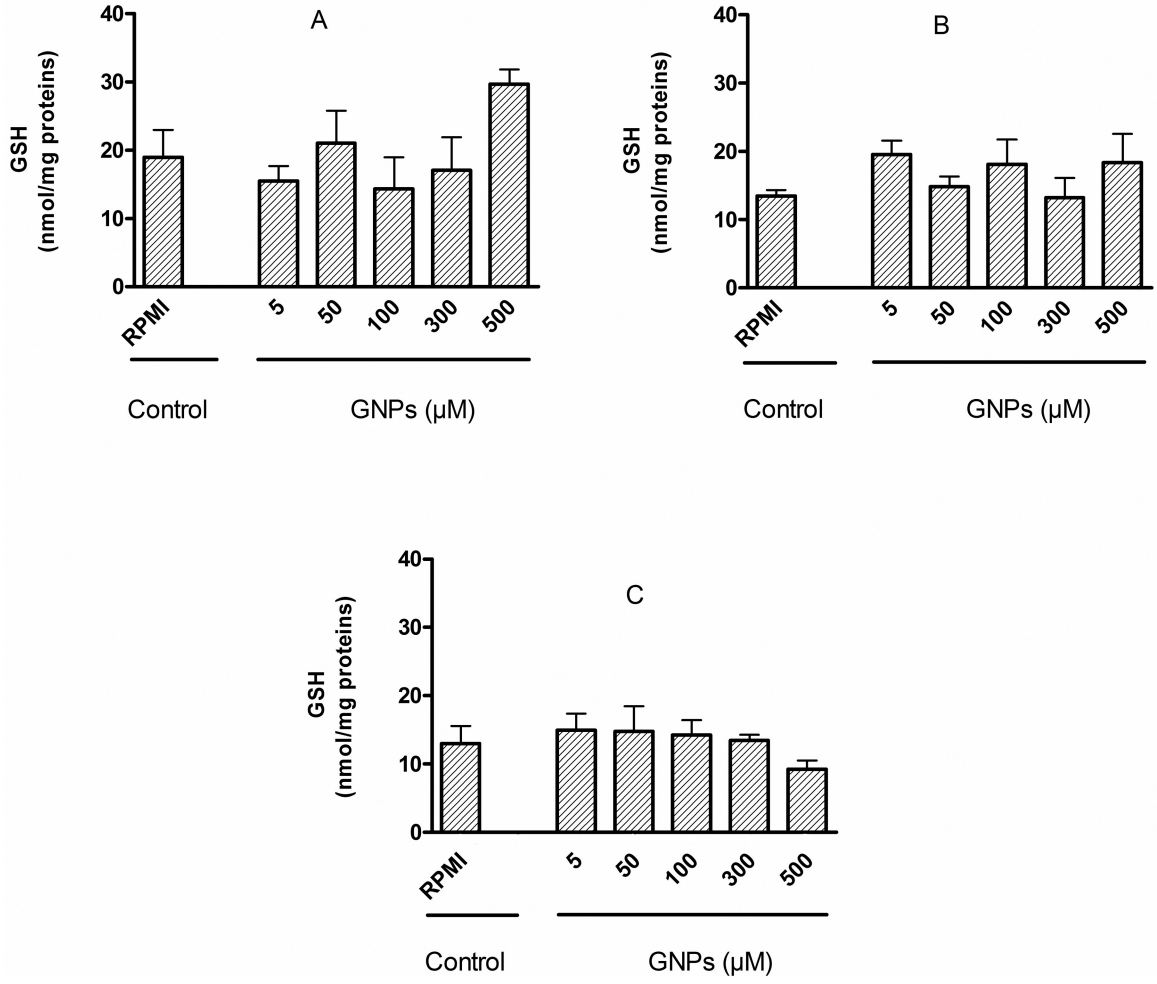

FIG. 2. GSH levels in cultured rat liver precision-cut slices in the presence of GNPs. Slices were incubated for various periods of time (2, 6, and 24 h) in the presence of different concentrations of GNPs (5–500μM) (panel A, B, and C). GSH content was measured in slice homogenates as reported in the Materials and Methods section. Columns marked RPMI represent slices cultured in the presence of RPMI alone as control conditions. Results are expressed as mean ± SEM of values obtained in triplicate from slices of liver of three animals.

TABLE 2
Reduced (GSH) and Oxidized (GSSG) Glutathione Levels in Cultured Rat Liver Precision-Cut Slices After Exposure to GNPs

Treatment	GSH (nmol × mg proteins^{-1})	GSSG (nmol × mg proteins^{-1})
[a]RPMI (0 h)	18.45 ± 1.01	1.08 ± 0.43
[b]RPMI (24 h)	12.99 ± 2.59	0.74 ± 0.13
GNP (5μM)	14.95 ± 2.42	0.76 ± 0.16
GNP (50μM)	14.81 ± 3.64	1.44 ± 0.36
GNP (100μM)	14.27 ± 2.21	1.06 ± 0.38
GNP (300μM)	13.49 ± 0.81	0.81 ± 0.31
GNP (500μM)	9.29 ± 1.33	1.03 ± 0.27

Note. Slices were incubated in the presence of different concentrations of GNPs coated with PVP (5–500μM) for 24 h, and GSH and GSSG contents were measured in slice homogenates as reported in the Materials and Methods section. RPMI represents slices cultured in the presence of RPMI alone as control conditions. Results are expressed as mean ± SEM of values obtained in triplicate from slices of liver of three animals.

[a]GSH and GSSG contents were measured after 0 h incubation in RPMI.

[b]GSH and GSSG content was measured after 24 h incubation in RPMI.

These results were further confirmed when CYP activities were measured by using marker substrates in microsomal preparations obtained from slices incubated for 24 h with GNPs at 500μM concentration. In this case, the activities of ethoxyresorufin-O-dealkylase (EROD, marker of CYP1A family), pentoxyresorufin-O-dealkylase (PROD, marker of CYP2B family), and benzyloxyresorufin-O-dealkylase (BROD, marker of CYP2B and 3A families) were not affected by GNPs (Fig. 4).

TEM Analysis of Liver Slices

In order to monitor the diffusion of GNPs across liver slices and their possible import in the cells from outside, TEM analysis of slices incubated for different times with either 5 or 500μM GNPs was performed. In some cases, identification of GNPs was facilitated by the silver enhancement procedure. Uptake of GNPs took place within the first 30-min incubation, with endocytotic vesicles containing GNPs being noted (Fig. 5A) at that time; this process was even more evident after 1 h, when silver-enhanced GNPs could be spotted in vesicles below the plasma membrane of the first layer of hepatocytes (Fig. 5B). After 2 h, GNPs were found inside large endosome-like vesicles deeply situated into the cytoplasm of hepatocytes, close to the Golgi complex (Fig. 5C), in several cases. After 4 h, silver-enhanced GNPs were observed inside endosomes, forming large aggregates of precipitated material (Figs. 5D and E), and after 6 h, GNPs were located close to the apical domain of hepatocytes (i.e., close to the biliary canaliculi) and also inside hepatocytes of the second layer (Figs. 5F and G). As the thickness of the slices encompassed on average 10 layers of cells and as the medium bathed both sides of the slices, the present results suggest that at least 40% of the liver cells interacted with GNPs. Control slices (medium alone or medium with either PVP or $AuCl_3$) were consistently negative as they did not display any silver precipitate (data not shown). We have also analyzed sections of slices not processed according to the silver enhancement protocol. In this way, it was possible to relieve the fine structure of the vesicles containing few GNPs. After 2 h incubation, more GNPs were found inside the vesicles (Supplementary fig. S4.A), and after 6 h, they were deep into the cytoplasm close to the Golgi complex or even inside multivesicular bodies (Supplementary fig. S4 B). After 24 h, the slice structure appeared well preserved, and the superficial layer of cells showed sustained uptake of GNPs (Supplementary fig. S4.C). GNPs were never observed inside nuclei or mitochondria.

Other cell types beside hepatocytes appeared to be capable of taking up GNPs. Kupffer cells appeared to be the most active cells in this process, with GNPs being taken up by them even at 50μM concentration (Fig. 6A). Endothelial cells of

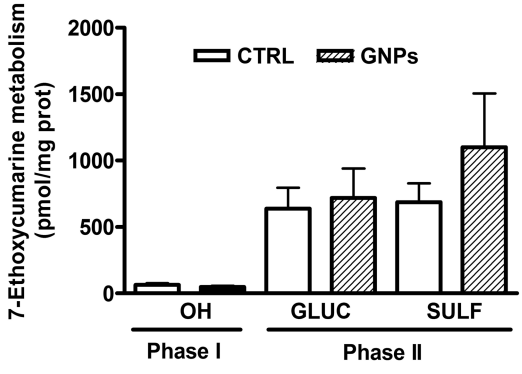

FIG. 3. 7-Ethoxycumarine dealkylase (OH), 7-hydroxycumarine glucuronyl (GLU)-transferase, and sulfo (SULPH)-transferase activities in rat liver precision-cut slices. Slices were incubated for 24 h with 500μM GNPs prior to the addition of 50μM 7-ethoxycumarine and subsequent incubation for 2 h. The amount of formed metabolites was measured in the culture medium. Results are expressed as mean ± SEM of three determinations from each of the four animals.

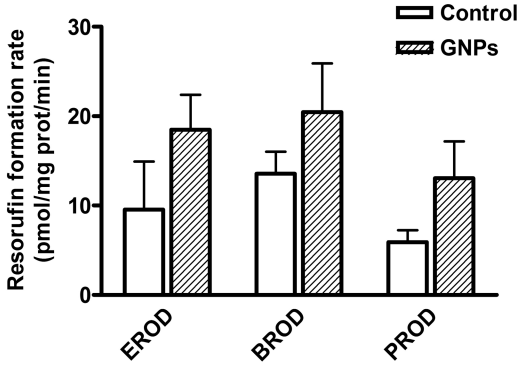

FIG. 4. Ethoxy-(EROD), benzyloxy-(BROD), and pentoxyresorufin O-deethylase (PROD) activities. Cytochrome P 450–dependent activities were assayed in the microsomal preparations obtained from rat liver precision-cut slices previously incubated for 24 h in presence of 500μM GNPs. Results are expressed as mean ± SEM of determinations on three different microsomal preparations from each of the four rat livers.

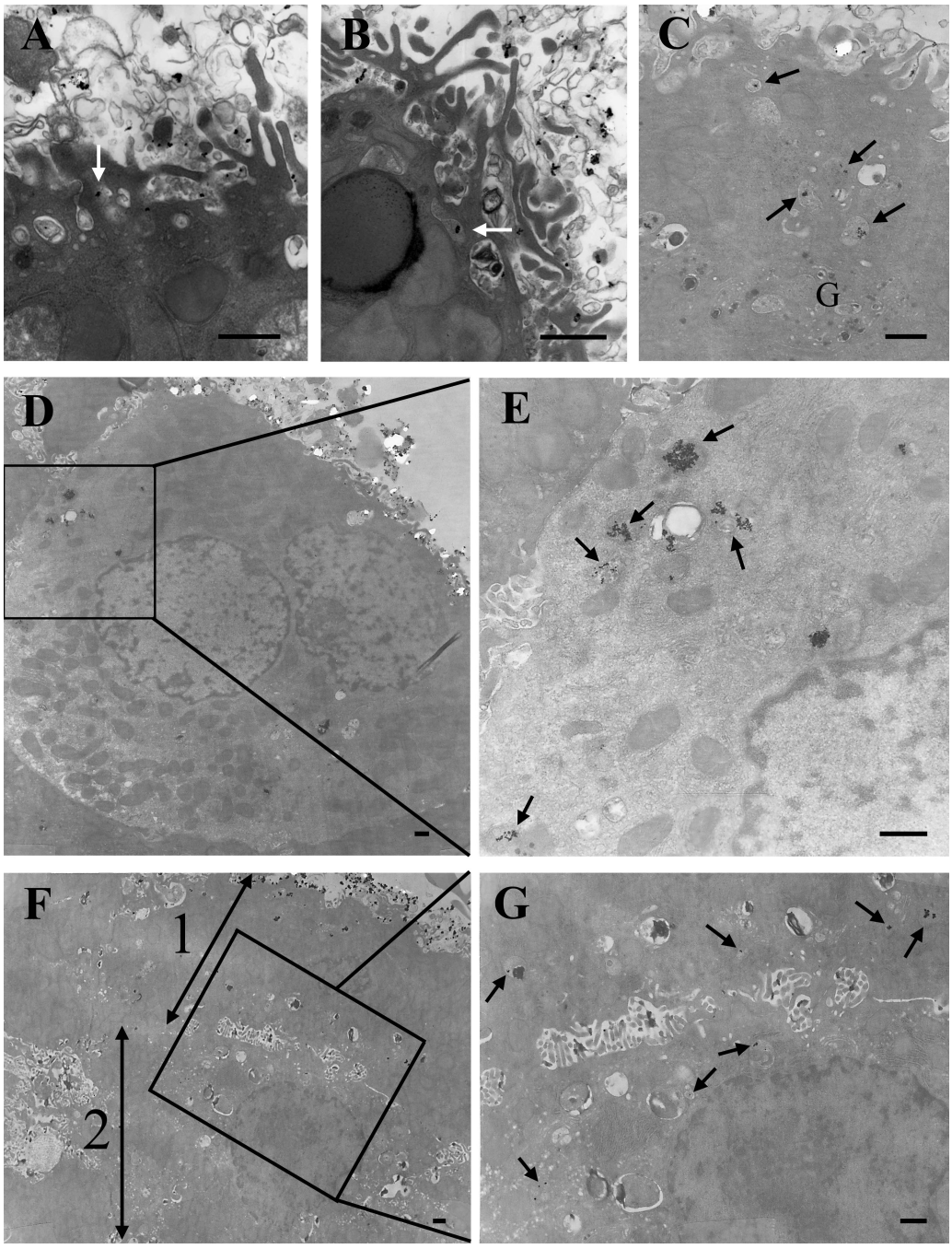

FIG. 5. Hepatocyte uptake of GNPs after various incubation times at 500μM concentration. Silver enhancement. Magnification bars = 0.5 μm. (A) 30 min of incubation. A vesicle, likely just formed, containing silver precipitate is visible (arrow); (B) 1 h of incubation. A vesicle containing the silver precipitate, which unveils uptaken colloidal GNP, is located below the hepatocyte plasma membrane (arrow); (C) 2 h of incubation. Silver precipitate is present within several endosome-like vesicles (arrows). Some of these vesicles are deep in the hepatocyte cytoplasm and reach the Golgi complex (G). (D and E) 4 h of incubation. A binucleated hepatocyte displays large aggregates of silver precipitates. (E) Higher magnification of the framed area in D. Some of the silver precipitate aggregates are highlighted with arrows. (F and G) 6 h of incubation. (F) Low magnification showing two (1 and 2) layers of well-preserved hepatocytes; (G) Higher magnification of the framed area in F. Silver precipitates (arrows) are present in cells of both layers close to a biliary canaliculus.

large venules (Fig. 6B) or collapsed sinusoids (Figs. 6C and D) were also capable of internalizing GNPs. This capability was also shared by mononuclear cells present in some blood vessels (Figs. 6D–G). Remarkably, GNPs were mostly adhering to the cell membrane of those mononuclear leukocytes located within large vessels (Figs. 6F and G). Liver stellate cells seemed not to perform this process as GNPs were never found in their cytoplasm.

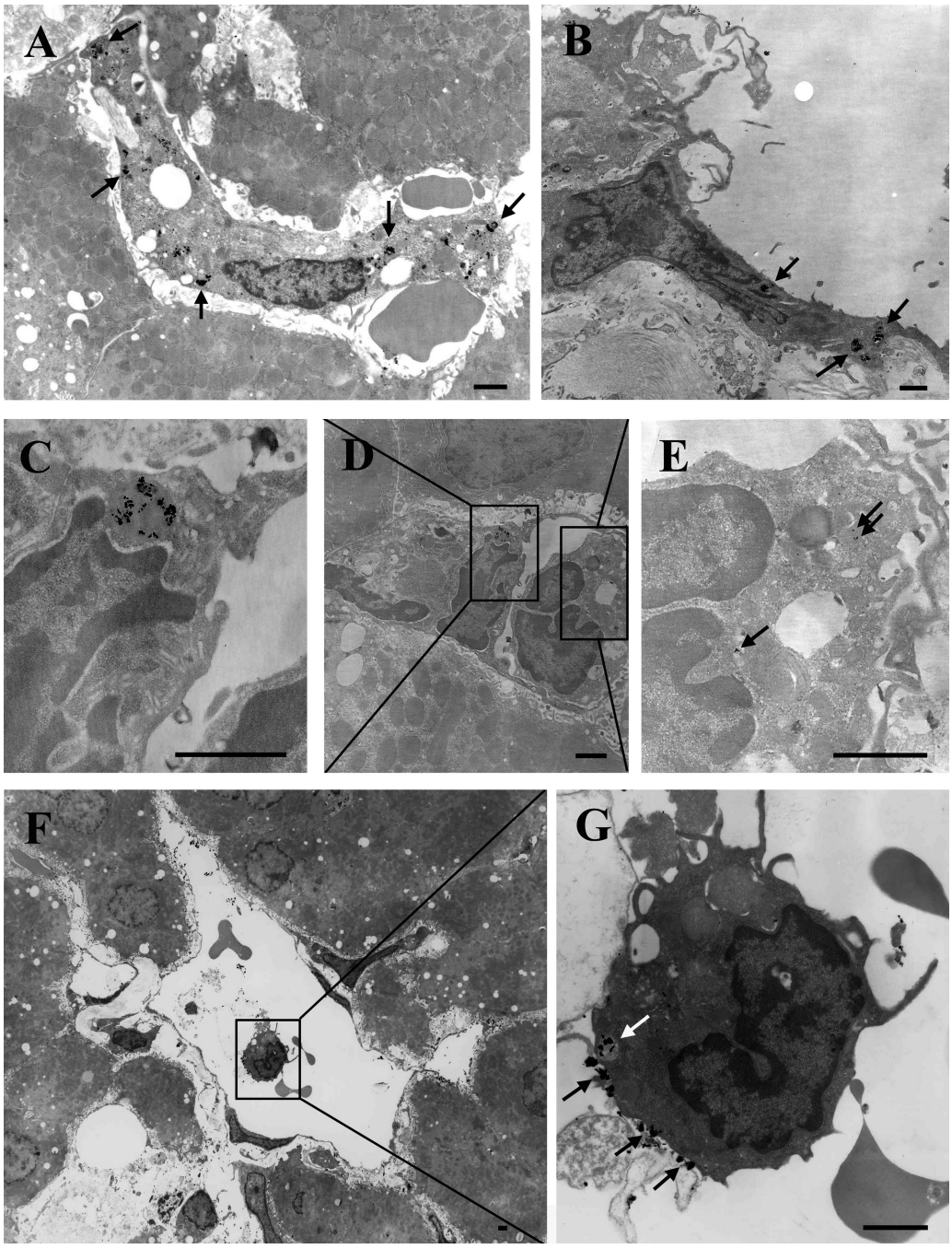

FIG. 6. Internalization of GNPs in cells other than hepatocytes. Magnification bars = 1 μm. (A–E) 24 h of incubation time. (A) A Kupffer cell shows several endosomes (arrows) containing silver-enhanced GNPs. GNP concentration: 50μM. (B) Endothelial cell outlining a large vessel. Three endosomes (arrows) contain silver-enhanced GNPs. GNP concentration: 50μM. (C–E) In D, a collapsed blood sinusoid is outlined by an endothelial cell and contains a mononuclear cells; C = higher magnification of the left framed area in D showing details of the endothelial cell. A large endosome containing silver-enhanced GNPs is visible close to the nucleus; E = higher magnification of the right framed area in D showing details of the mononuclear cell. Few silver-enhanced NPs are visible inside cytoplasmic vesicles (arrows). GNP concentration: 500μM. (F) 3 h of incubation with 500μM GNPs. Low magnification of a centrilobular vein. The parenchyma surrounding the vein is well preserved and a mononuclear cell is visible at the centre of the venule. (G) Higher magnification of the framed area in F. Inside the mononuclear cell, an endosome is filled with silver-enhanced GNPs. Several large aggregates of silver precipitates are attached to the membrane of the mononuclear cell.

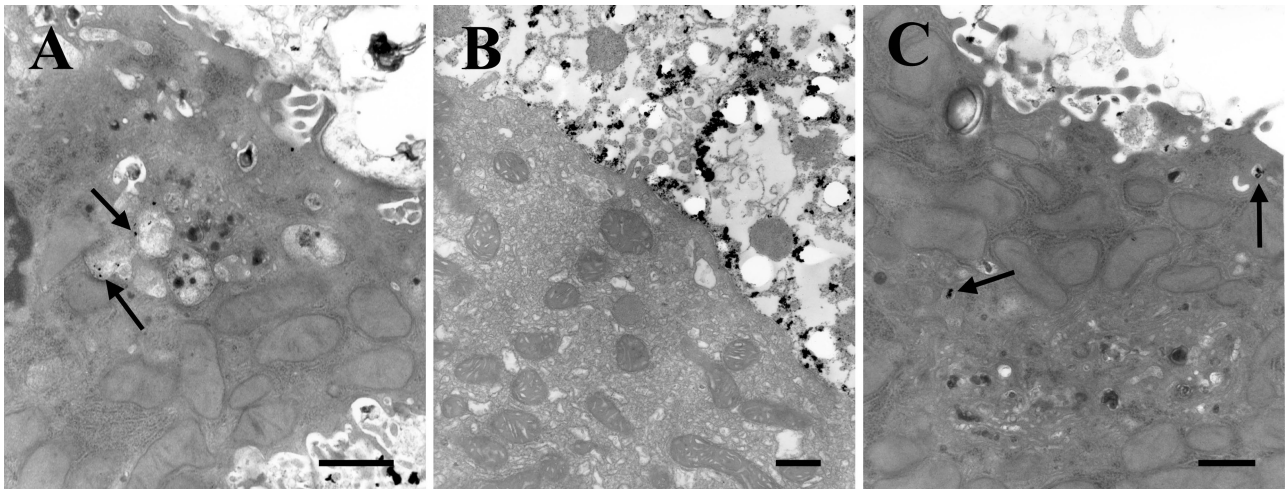

FIG. 7. Temperature-dependent internalization of GNPs by hepatocytes of precision-cut liver slices. Slices incubated with 500μM GNPs. Silver enhancement. Magnification bars = 0.5 μm. (A) 3 h of incubation at 37°C. Silver precipitates are within endosome-like vesicles (arrows). (B) 3 h of incubation at 4°C. Silver precipitates are visible only outside the hepatocytes. The cytoplasm shows several distended vesicles some of them are cisterns of rough endoplasmic reticulum. (C) 3 h of incubation at 4°C followed by 3 h of incubation at 37°C. Cell morphology and cell capability to take up GNPs (arrows) are completely restored.

In order to assess whether internalization of GNPs was an active phenomenon, some liver slices were incubated with GNPs at 4°C for 3 h, whereas other slices were incubated in parallel at 37°C, as controls. As expected, hepatocytes of slices incubated at 37°C internalized GNPs (Fig. 7A); in contrast, cells of slices incubated at 4°C did not show any internalization of GNPs (Fig. 7B). After incubation at 4°C, the cytoplasm showed several enlarged membranous compartments like the cisterns of the rough endoplasmic reticulum that appeared larger than normal. However, these modifications were reversible, and when liver slices were switched again at 37°C for a further 3 h, a normal cell morphology was displayed, along with the ability of the cell to take up GNPs (Fig. 7C).

TABLE 3
Gold Level in Rat Liver and Bile After Both *In Vivo* and *In Vitro* Treatment

Treatment	Amount of gold used to treat (μg)	Concentration of gold found in tissue (μg × g^{-1})	Total gold found in tissue (μg)	Recovery (%)
Precision cut slices[a] (50μM)	7.35	18.69	0.5	6.80
Precision cut slices[a] (500μM)	73.50	61.01	1.5	2.04
Liver[b]	2500.00[b]	19.82	305.3	12.20
Bile[c]	2500.00[b]	73.00[c]	1.0	0.04

[a]The two concentrations in the assay corresponded to 9.8 and 98 μg gold × ml^{-1} of culture medium, respectively.

[b]The *in vivo* acute treatment consisted in injecting ip a GNP dose corresponding to 10 mg gold × kg^{-1} body weight to rats.

[c]Total amount of gold recovered in 14 ml of bile collected from 6 to 12 h after the *in vivo* treatment.

In Vivo Experiments

In order to verify whether the results obtained with liver slices were representative of what may occur *in vivo*, we performed *in vivo* experiments by injecting ip a GNP suspension (see Materials and Methods). TEM analysis of liver fragments taken 12 h post injection showed the presence of GNPs inside hepatocytes. In particular, GNPs could be spotted within multivesicular bodies (Fig. 8A) and dense lysosomes (Fig. 8B). Interestingly, GNPs were always proximal to the apical pole of the hepatocytes. In addition, confirming the *in vitro* results, GNPs were also found inside endothelial and Kupffer cells (Fig. 8C).

ICP-OES analysis showed that the amount of gold present in the liver 12 h after treatment corresponded to 12% of the injected gold. In the bile obtained from rats treated with GNPs and collected between 6 and 12 h after treatment, the amount of gold corresponded to a mere 0.04% of the total amount of gold injected and to 0.32% of the total gold present in the liver 12 h after treatment, thus suggesting that liver, although slowly, is able to dispose GNPs through the bile excretory system (see Table 3).

DISCUSSION

Because the number of NMs engineered for industrial purposes or medical applications is rapidly growing, the large diffusion of substances sharing this size scale is a highly potential source of risks for the human health and the environment. Paradoxically, in most cases, risks cannot be weighted correctly owing to the large amount of conflicting studies; in general, at the root of these conflicts is the large number of different experimental model systems employed, which makes it difficult to compare and interpret the results. As to NM risk assessment, it is important to consider the

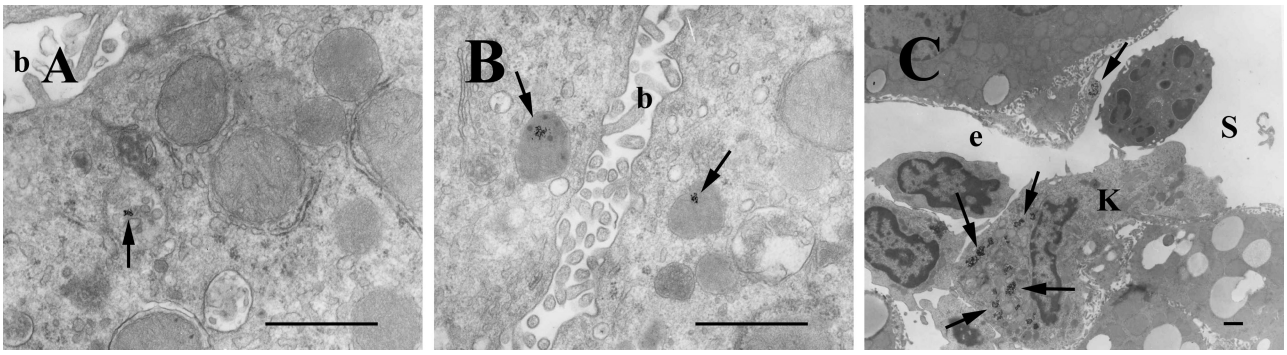

FIG. 8. *In vivo* uptake by liver cells of GNPs after single ip administration of GNPs. Magnification bars = 0.5 μm. (A) GNPs (arrow) are visible within a multivesicular body (late endosome) located close to a biliary canaliculus (b). (B) Two hepatocytes outlining the opposite sides of a biliary canaliculus (b) are provided with dense lysosomes containing GNPs (arrows). (C) A Kupffer cell (K) protruding into a sinusoid capillary (S) shows a great number of endosomes containing aggregates of GNPs (arrows). Even the sinusoid endothelial cell (e) displays a large endosome engulfed with GNPs (arrow).

unique physicochemical characteristics of each NP, the various routes of entry of NP into the human body or into other organisms, the biological activity of NP, and the target organs of NP. It is important to stress that, regardless of the route by which the exposure takes place, NPs appear capable of spreading throughout the body (Semmler-Benhke *et al.*, 2008). According to several observations, liver is one of the main sites where NMs can translocate and accumulate, regardless of their chemical and physical structure (i.e., gold, silica, NPs, quantum dots, and nanotubes) (Balasubramanian *et al.*, 2010; Fischer *et al.*, 2006; Kumar *et al.*, 2010; Schipper *et al.*, 2008).

These considerations prompted us to investigate whether PVP-coated, 5 nm GNPs affect liver biology, by employing precision-cut slices as an *in vitro* model system to study the toxicity of GNPs toward liver cells and their uptake by liver cells.

Our results indicate that these GNPs did not promote toxic effects on hepatic tissue. These data are in accordance with the results presented by other authors who used primary cultures of hepatocytes or the hepatoma cell line HepG2 as an *in vitro* model system (Khlebtsov and Dykman, 2011; Ponti *et al.*, 2009). However, contrasting results have been provided, which suggest that toxicity of GNPs appears to be related to the choice of the coating materials and/or to their size (Pan *et al.*, 2007; Pan *et al.*, 2009). In particular, Pan *et al.* (2007) found that 1.4-nm GNPs capped with triphenylphosphine monosulfonate were much more cytotoxic than 15-nm GNPs capped with the same material. However, because 1.4-nm GNPs capped with GSH resulted markedly less cytotoxic, they concluded that the toxicity of small GNPs depends on their ability to trigger the intracellular formation of ROS from dioxygen (Pan *et al.*, 2009).

The present results, however, tell a different story as no evidence of oxidative stress could be obtained in precision-cut liver slices; indeed, a reduction of about 30% of GSH content was observed after 2 or 24 h of incubation with GNPs, but this decrease was also observed in control slices. This was confirmed by the observation that the concentration of GSSG was not statistically different in control and GNP-treated slices.

Due to the presence of the high levels of xenobiotic metabolizing enzymes, liver is the major organ devoted to the detoxification function. As the interference with the xenobiotic metabolizing system could be the cause of indirect toxicity, it was important to evaluate the effect of GNPs on different enzyme activities related to this system. Under the present experimental conditions, incubation of liver precision-cut slices for 24 h with 500μM GNPs did not modify either the activity of CYPs or the conjugative enzymes assayed. These results were in contrast with those reported by Fröhlich *et al.* (2010), showing that polystyrene NPs can inhibit CYP-dependent xenobiotic metabolism. However, they tested the effects of polystyrene nanobeads on a cell-free system consisting of the microsomal fraction isolated from transfected insect cells or endothelial and hepatoma cells. This direct interaction of NPs with microsomes is highly unlikely to occur in intact cells, as NPs are usually sequestered inside the organelles of the endocytotic pathway.

In order to ascertain whether the absence of toxicity in our experimental model could be due to a limited access of GNPs into the cells, we carried out a careful TEM analysis of liver precision-cut slices exposed to GNPs. Our results showed that in this *in vitro* model system GNPs had full access to all cell types present in liver. In particular, GNPs were actively taken up by Kupffer cells, blood endothelial cells, blood mononuclear cells, and hepatocytes. Our experimental model can be considered reliably representative of what occurs *in vivo* upon GNP exposure as the same results were obtained after ip administration of GNPs.

The ability of liver to take up NPs has been known for a long time. The cells primarily involved in this uptake process are mainly Kupffer cells that seem capable of internalizing NPs of various diameters and composition, regardless of their coating (Cho *et al.*, 2009; Choi *et al.*, 2010; Ogawara *et al.*, 1999; Sadauskas *et al.*, 2007). Even blood vessel endothelial cells have been reported to take up NPs of different chemical composition, though less frequently (Kanai *et al.*, 1996; Ogawara *et al.*, 1999). However, the ability of hepatocytes to internalize NPs and, more specifically, GNPs is still debated.

In spite of numerous toxicological studies carried out on the hepatoma cell line HepG2 (Khlebtsov and Dykman, 2011 and references therein), only a few *in vitro* studies using cell cultures have addressed attention to the ability of hepatocytes to internalize GNPs or polystyrene NPs (Deschuyteneer *et al.*, 1984; Kolb-Bachofen *et al.*, 1984; Johnstone *et al.*, 2010; Ponti *et al.*, 2009; Tkachenko *et al.*, 2004). Although NP preparations were consistently different in terms of functionalization, size, and chemical composition, NPs were taken up inside the cells in all cases. In addition, some GNPs were reported to get into the nuclei of HepG2 cells (Tkachenko *et al.*, 2004), whereas 20-nm polystyrene NPs were claimed to get access into the mitochondria (Johnstone *et al.*, 2010). However, in both cases incontrovertible, direct evidence was not supplied. On the other hand, all of these studies were conducted on 2D cell cultures, and the toxicological feature of the NP employed could be different from that displayed in 3D cultures (Lee *et al.*, 2009).

Moreover, preliminary experiments have showed that naked GNPs of different sizes (5–80 nm) were toxic in a size-dependent fashion either on liver slices or on HepG2 cells incubated for 24 h. In particular, 5- and 15-nm naked GNPs promoted a significant decrease of the ability to reduce MTT in both *in vitro* model systems (Dragoni, personal communication). These data were in accordance with those reported by several authors demonstrating that naked GNPs are harmful to liver both in *in vivo* and *in vitro* conditions (for a review, see Sabella *et al*., 2011).

ICP-OES gold determination showed that both the precision-cut rat liver slices *in vitro* and the liver *in vivo* upon ip administration take up GNPs consistently. In fact, the recovery of Au in the slices after 24 h incubation with 5μM GNPs amounted to 6% of the Au present in the incubation medium, whereas the percentage found in the liver resulted to be 12% of the dose injected (see Table 3). For this reason, under our experimental conditions, we inferred that precision-cut liver slices were representative of what happens *in vivo*. Inside the hepatocytes, PVP-coated GNPs were never observed within mitochondria or nuclei but were always limited to uncoated vesicles, early endosome-like vesicles, late endosomes, and lysosomes located close to the biliary canaliculi. To our knowledge, import of GNPs along the entire endocytotic pathway of the hepatocyte has been previously reported only in 2D cultures using GNPs coated with galactosylated bovine serum albumin interacting with the asialoglycoprotein receptor (Deschuyteneer *et al.*, 1984), or fluid phase markers GNPs (Lake *et al.*, 1987). Indeed, GNPs functionalized with various ligands frequently used to probe the presence of specific receptors and to track the intracellular path ligands were internalized by coated vesicles inside hepatocytes (Deschuyteneer et al., 1984; Gebhardt and Robenek, 1987).

The ability of hepatocytes to take up NPs in *in vivo* conditions is still debated. In fact, recent studies employing polyethylene glycol-coated or apparently nonfunctionalized GNPs seem to rule out this capability (Cho *et al.*, 2009; Sadauskas *et al.*, 2009). On the other hand, our own results confirm those of previous studies that hepatocytes are capable of taking up *in vivo* a large variety of NPs (Choi *et al.*, 2010; Hardonk *et al.*, 1985; Kanai *et al.*, 1996; Ogawara *et al.*, 1999) and provide the evidence that uptake of GNPs by the hepatocyte takes place through the endosomal pathway up to dense lysosomes clustered around the biliary canaliculi.

CONCLUSIONS

Under the present conditions, GNPs did not exhibit signs of acute toxicity toward hepatocytes even after 24 h of exposure to them. Five-nanometer GNPs stabilized with PVP are easily taken up by blood vessel endothelial cells, Kupffer cells, and hepatocytes either *in vitro*, in precision-cut rat liver slices, or *in vivo*. The match of behavior of GNPs *in vivo* and in rat liver precision-cut slices underlined by histological analysis suggests the latter as a possible sound technique for studying liver toxicity of NPs.

SUPPLEMENTARY DATA

Supplementary data are available online at http://toxsci.oxfordjournals.org/.

FUNDING

Istituto Toscano Tumori, Regione Toscana, Firenze, Italy.

ACKNOWLEDGMENTS

The authors thank Prof. F. De Matteis for critical reading of the manuscript.

REFERENCES

Balasubramanian, S. K., Jittiwat, J., Manikandan, J., Ong, C., Yu, L. E., and Ong, W. (2010). Biodistribution of gold nanoparticles and gene expression changes in the liver and spleen after intravenous administration in rats. *Biomaterials* **31,** 2034–2042.

Cho, W. S., Cho, M., Jeong, J., Choi, M., Cho, H-Y., Han, B. S., Kim, S. H., Kim, H. O., Lim, Y. T., Chung, B. H., *et al*. (2009). Acute toxicity and pharmacokinetics of 13 nm-sized PEG-coated gold nanoparticles. *Toxicol. Appl. Pharmacol.* **236,** 16–24.

Choi, C. H. J., Alabi, C. A., Webster, P., and Davis, M. E. (2010). Mechanism of active targeting in solid tumors with transferrin-containing gold nanoparticles. *Proc. Natl. Acad. Sci. U.S.A.* **107,** 1235–1240.

de Graaf, I. A., Olinga, P., de Jager, M. H., Merema, M. T., de Kanter, R., van de Kerkhof, E. G., and Groothuis, G. M. (2010). Preparation and incubation of precision-cut liver and intestinal slices for application in drug metabolism and toxicity studies. *Nat. Protoc.* **5,** 1540–1551.

Deschuyteneer, M., Prieels, J. P., and Mosselmans, R. (1984). Galactose-specific adsorptive endocytosis: An ultrastructural qualitative and quantitative study in cultured rat hepatocytes. *Biol. Cell* **50,** 17–29.

Dragoni, S., Materozzi, G., Pessina, F., Frosini, M., Marco, J. L., Unzeta, M., Sgaragli, G., and Valoti, M. (2007). CYP-dependent metabolism of

PF9601N, a new monoaminooxidase-B inhibitor, by C57BL/6 mouse and liver human microsomes. *J. Pharm. Pharm. Sci.* **10,** 473–485.

Fischer, H. C., Liu, L., Pang, K. S., and Chan, W. C. W. (2006). Pharmacokinetics of nanoscale quantum dots: In vivo distribution, sequestration, and clearance in the rat. *Adv. Funct. Mater.* **16,** 1299–1305.

Fröhlich, E., Kueznik, T., Samberger, C., Roblegg, E., Wrighton, C., and Pieber, T. R. (2010). Size-dependent effects of nanoparticles on the activity of cytochrome P450 isoenzymes. *Toxicol. Appl. Pharmacol.* **242,** 326–332.

Gay, R. J., McComb, R. B., and Bowers, G. N. Jr. (1968). Optimum reaction conditions for human lactate dehydrogenase isoenzymes as they affect total lactate dehydrogenase activity. *Clin. Chem.* **14,** 740–753.

Gebhardt, R., and Robenek, H. (1987). Ligand-dependent redistribution of the IgA receptor on cultured rat hepatocytes and its disturbance by cytochalasin B. *J. Histochem. Cytochem.* **35,** 301–309.

Griffith, L. G., and Swartz, M. A. (2006). Capturing complex 3D tissue physiology *in vitro*. *Nat. Rev. Mol. Cell Biol.* **7,** 211–224.

Hardonk, M. J., Harms, G., and Koudstaal, J. (1985). Zonal heterogeneity of rat hepatocytes in the *in vivo* uptake of 17 nm colloidal gold granules. *Histochemistry* **83,** 473–477.

Hui, A. Y., and Friedman, S. L. (2003). Molecular basis of hepatic fibrosis. *Expert. Rev. Mol. Med.* **5,** 1–23.

Jia, H. Y., Liu, Y., Zhang, X. J., Han, L., Du, L. B., Tian, Q., and Xu, Y. C. (2009). Potential oxidative stress of gold nanoparticles by induced-NO releasing in serum. *J. Am. Chem. Soc.* **131,** 40–41.

Johnstone, H. J., Semmler-Behnke, M., Brown, D. M., Kreyling, W., Tran, L., and Stone, V. (2010). Evaluating the uptake and intracellular fate of polystyrene nanoparticles by primary and hepatocytes cell lines *in vitro*. *Toxicol. Appl. Pharmacol.* **242,** 66–78.

Kanai, M., Murata, Y., Mabuchi, Y., Kawahashi, N., Tanaka, M., Ogawa, T., Doi, M., Soji, T., and Herbert, D. C. (1996). *In vivo* uptake of lecithin-coated polystyrene beads by rat hepatocytes and sinusoidal endothelial cells. *Anat. Rec.* **244,** 175–181.

Khlebtsov, N., and Dykman, L. (2011). Biodistribution and toxicity of engineered gold nanoparticles: A review of *in vitro* and *in vivo* studies. *Chem. Soc. Rev.* **40,** 1647–1671.

Kolb-Bachofen, V., Schlepper-Schäfer, J., Roos, P., Hülsmann, D., and Kolb, H. (1984). GalNAc/Gal-specific rat liver lectins: Their role in cellular recognition. *Biol. Cell* **51,** 219–226.

Kumar, R., Roy, I., Ohulchanskky, T. Y., Vathy, L. A., Bergey, E. J., Sajjad, M., and Prasad, P. M. (2010). *In vivo* biodistribution and clearance studies using multimodal organically modified silica nanoparticles. *ACS Nano.* **4,** 699–708.

Lake, J. R., Van Dyke, R. W., and Scharschmidt, B. F. (1987). Acidic vesicles in cultured rat hepatocytes. Identification and characterization of their relationship to lysosomes and other storage vesicles. *Gastroenterology* **92,** 1251–1261.

Lee, J., Lilly, G. D., Doty, R. C., Podsiadlo, P., and Kotov, N. A. (2009). *In vitro* toxicity testing of nanoparticles in 3D cell culture. *Small* **10,** 1213–1221.

Lewinski, N., Colvin, V., and Drezek, R. (2008). Cytotoxicity of nanoparticles. *Small* **4,** 26–49.

Li, J. J., Hartono, D., Ong, C. N., Bay, B. H., and Yung, L. Y. (2010). Autophagy and oxidative stress associated with gold nanoparticles. *Biomaterials* **31,** 5996–6003.

Liu, X., Atwater, M., Wang, J., and Huo, Q. (2007). Extinction coefficient of gold nanoparticles with different sizes and different capping ligands. *Colloids Surf. B Biointerfaces* **58,** 3–7.

Mohammed, F. F., and Khokha, R. (2005). Thinking outside the cell: Proteases regulate hepatocyte division. *Trends Cell. Biol.* **15,** 555–563.

Moronvalle-Halley, V., Sacré-Salem, B., Sallez, V., Labbe, G., and Gautier, J. C. (2005). Evaluation of cultured, precision-cut rat liver slices as a model to study drug-induced liver apoptosis. *Toxicology* **207,** 203–214.

Ogawara, K., Yoshhida, M., Higaki, K., Kimura, T., Shiraishi, K., Nishikawa, M., Takakura, Y., and Hashida, M. (1999). Hepatic uptake of polystyrene microsphere in rats: Effect of particle size on intrahepatic distribution. *J. Contr. Rel.* **59,** 15–22.

Olinga, P., Merema, M. T., de Jager, M. H., Derks, F., Melgert, B. N., Moshage, H., Slooff, M. J., Meijer, D. K., Poelstra, K., and Groothuis, G. M. (2001). Rat liver slices as a tool to study LPS-induced inflammatory response in the liver. *J. Hepatol.* **35,** 187–194.

Onderwater, R. C., Commandeur, J. N., and Vermeulen, N. P. (2004). Comparative cytotoxicity of N-substituted N'-(4-imidazole-ethyl)thiourea in precision-cut rat liver slices. *Toxicology* **197,** 81–91.

Pan, Y., Leifert, A., Ruau, D., Neuss, S., Bornemann, J., Schmid, G., Brandau, W., Simon, U., and Jahnen-Dechent, W. (2009). Gold nanoparticles of diameter 1.4 nm trigger necrosis by oxidative stress and mitochondrial damage. *Small* **5,** 2067–2076.

Pan, Y., Neuss, S., Leifert, A., Fischler, M., Wen, F., Simon, U., Schmid, G., Brandau, W., and Jahnen-Dechent, W. (2007). Size-dependent cytotoxicity of gold nanoparticles. *Small* **3,** 1941–1949.

Ponti, J., Colognato, R., Franchini, F., Gioria, S., Simonelli, F., Abbas, K., Uboldi, C., Kirkpatrick, J., Holzwarth, U., and Rossi, F. (2009). A quantitative *in vitro* approach to study the intercellular fate of gold nanoparticles: From synthesis to cytotoxicity. *Nanotoxicology* **3,** 296–306.

Sabella, S., Galeone, A., Vecchio, G., Cingolani, R., and Pompa, P. P. (2011). AuNPs are toxic in vivo and in vitro: A review. *J. Nanosci. Lett.* **1,** 145–165.

Sadauskas, E., Danscher, G., Stoltenberg, M., Vogel, U., Larsen, A., and Wallin, H. (2009). Protracted elimination of gold nanoparticles from mouse liver. *Nanomed: Nanotechnol. Biol. Med.* **5,** 162–169.

Sadauskas, E., Wallin, H., Stoltenberg, M., Vogel, U., Doering, P., Larsen, A., and Danscher, G. (2007). Kupffer cells are central in the removal of nanoparticles from the organism. *Part. Fibre Toxicol.* **4,** 10.

Savolainen, K., Alenius, H., Norppa, H., Pylkkänen, L., Tuomi, T., and Kasper, G. (2010). Risk assessment of engineered nanomaterials and nanotechnologies—A review. *Toxicology* **269,** 92–104.

Schipper, M. L., Nakayama-Ratchford, N., Davis, C. R., Kam, N. W. S., Chu, P., Liu, Z., Sun, X., Dai, H., and Gambhir, S. S. (2008). A pilot toxicology study of single-walled carbon nanotubes in a small sample of mice. *Nat. Nanotechnol.* **3,** 216–221.

Semmler-Behnke, M., Kreyling, W. G., Lipka, J., Fertsch, S., Wenk, A., Takenaka, S., Schmid, G., and Brandau, W. (2008). Biodistribution of 1.4- and 18-nm gold particles in rats. *Small* **4,** 2108–2111.

Tarantola, M., Pietuch, A., Schneider, D., Rother, J., Sunnick, E., Rosman, C., Pierrat, S., Sönnichsen, C., Wegener, J., and Janshoff, A. (2011). Toxicity of gold-nanoparticles: Synergistic effects of shape and surface functionalization on micromotility of epithelial cells. *Nanotoxicology* **5,** 254–268.

Tkachenko, A. G., Xie, H., Liu, Y., Coleman, D., Ryan, J., Glomm, W. R., Shipton, M. K., Franzen, S., and Feldheim, D. L. (2004). Cellular trajectories of peptide-modified gold particle complexes: Comparison of nuclear localization signals and peptide transduction domains. *Bioconjug. Chem.* **15,** 482–490.

Turkevich, J., Stevenson, P. C., and Hillier, J. (1951). A study of the nucleation and growth processes in the synthesis of colloidal gold. *Discuss. Faraday Soc.* **11,** 55–75.

Vickers, A. E. (2009). Tissue slices for the evaluation of metabolism-based toxicity with the example of diclofenac. *Chem. Biol. Interact.* **179,** 9–16.

Yang, H., Liu, C., Yang, D., Zhang, H., and Xi, Z. (2009). Comparative study of cytotoxicity, oxidative stress and genotoxicity induced by four typical nanomaterials: The role of particle size, shape and composition. *J. Appl. Toxicol.* **29,** 69–78.